Sensors and Materials, Vol. 38, No. 2 (2026) 553–558
MYU Tokyo

S & M 4320

Evaluation of Scintillation Properties of LiBr:Yb for Thermal Neutron Detection

Keiichiro Miyazaki,* Daisuke Nakauchi, Takumi Kato, Noriaki Kawaguchi, and Takayuki Yanagida

Nara Institute of Science and Technology, 8916-5 Takayama, Ikoma, Nara 630-0192, Japan

(Received October 21, 2025; accepted December 16, 2025)

Keywords: scintillator, neutron detection, Bridgman-Stockbarger method, α/γ ratio

Scintillation properties of LiBr:Yb synthesized by the vertical Bridgman–Stockbarger method were investigated. Two emission peaks were observed at 415 and 450 nm under X-ray irradiation, which would be attributed to spin-allowed and spin-forbidden 5d–4f transitions of Yb^{2+}, respectively. According to pulse height spectra, the highest light yield values (*LY*) were 3500 photons/neutron and 1900 photons/MeV under ^{252}Cf neutron and ^{137}Cs γ-ray irradiation, respectively, and the α/γ ratio was 0.38. Although the *LY* was lower than that of the commercial Li-glass scintillator (GS20), the α/γ ratio was comparable to or higher than that of GS20.

1. Introduction

Neutron detectors have been used in security,[1] medicine,[2] and well-logging.[3] Since the September 11th terrorist attacks in 2001, the demand has rapidly increased in the security field to prevent nuclear terrorism and nuclear proliferation.[4] As conventional neutron detectors, ^3He proportional counters have been utilized.[5] ^3He is generated through the decay of tritium, and the depletion of ^3He has become a major issue due to nuclear disarmament and the prohibition of nuclear testing.[6] Against this background, scintillators for neutron detection have been required as an alternative detector of ^3He proportional counters.

Scintillators are a type of phosphor that can convert ionizing radiation to numerous photons with low energy, and ionizing radiation can be detected by coupling scintillators with photodetectors. To date, scintillators have been developed in various material forms such as single crystals,[7–14] ceramics,[15,16] and glasses,[17–21] and single crystals have been mainly focused on because of their high light yield (*LY*). In scintillators for neutron detection, the following properties are required: high *LY*, large cross section for neutron capture, non-hygroscopicity, and so forth. In addition, X- and γ-rays are generally generated in neutron irradiation fields. To reduce the sensitivity to X- and γ-rays, a small effective atomic number and a large α/γ ratio are required. Thus far, many ^6Li-based scintillators have been developed because of their high *Q*-value (4.78 MeV).[22–25] Among them, the following scintillators have been commercialized: LiF/ZnS:Ag,[26] Li-glass (GS20),[27] Cs_2LiYCl_6:Ce,[28] LiI:Eu,[29] and

*Corresponding author: e-mail: miyazaki.keiichiro.mg5@ms.naist.jp
https://doi.org/10.18494/SAM6019

ISSN 0914-4935
https://myukk.org/

$LiCaAlF_6$:Eu.[30] However, these scintillators do not fully satisfy all the requirements, and new scintillators for neutron detection are required.

LiBr is one of the promising hosts of scintillators for neutron detection because of its high Li concentration and small Z_{eff} compared with LiI (Z_{eff} = 34 for LiBr and 52 for LiI). Therefore, we focused on LiBr:Eu, and the scintillation properties were evaluated.[31] Although the luminescence due to 5d–4f transitions of Eu^{2+} was observed, the *LY* was 4600 photons/neutron (ph/n) under ^{252}Cf neutron irradiation, which is lower than those of commercial scintillators for neutron detection. In addition, the decay time constant due to 5d–4f transitions of Eu^{2+} was relatively long. Therefore, we focused on Yb^{2+}, which is known to show luminescence due to 5d–4f transitions, similar to Eu^{2+}, and there are two types of luminescence due to spin-allowed and spin-forbidden transitions.[32] In previous studies, Yb^{2+}-doped scintillators have been reported to show high *LY*.[33–35] In addition, the decay time constants of several tens of ns have been reported in Yb^{2+}-doped alkali halides.[36–39] Therefore, the scintillation properties of LiBr:Yb grown by the vertical Bridgman–Stockbarger method were evaluated in this study.

2. Experimental Methods

LiBr single crystals doped with 0.01, 0.03, 0.1, and 0.3% Yb were synthesized by the vertical Bridgman–Stockbarger method. $LiBr{\cdot}H_2O$ (3N, High Purity Chemicals) and $YbBr_3$ (3N, High Purity Chemicals) were mixed in the stoichiometric ratio. These powders were put into a quartz tube and dried at 300 ºC for 3 h in vacuum to remove moisture. Then, the quartz tube was sealed using a gas burner[40] and grown in a Bridgman furnace (VFK-1800, Crystal Systems). The temperature of the furnace was 600 ºC, and the pull-down speed was 5 mm/h. After growth, the quartz tubes were crushed to obtain the samples, and the obtained samples were polished to a thickness of 1–1.5 mm using sandpaper. Scintillation spectra under X-ray irradiation were measured using our original setup.[41] Scintillation decay profiles under pulse X-ray irradiation were obtained with an X-ray-induced afterglow characterization system.[42] To estimate *LY*, pulse height spectra were measured using a photomultiplier tube (PMT; R7600U-200, Hamamatsu Photonics) under ^{252}Cf neutron irradiation.[41] Moreover, pulse height spectra were measured under γ-ray irradiation from a ^{137}Cs source to evaluate the α/γ ratio.

3. Results and Discussion

The appearance of all the samples is shown in Fig. 1. All the samples were colorless and transparent. Scintillation spectra under X-ray irradiation of LiBr:Yb are shown in Fig. 2, and the inset shows the scintillation spectrum of the 0.01% Yb-doped sample. The 0.01% Yb-doped sample showed almost the same spectral shape as the undoped LiBr.[31] In the undoped LiBr, the possible emission origins were considered to be self-trapped excitons or intrinsic luminescence such as lattice defects and oxygen impurities. Therefore, the emission origin of the 0.01% Yb-doped sample was probably the same as that of the undoped one. In the other samples, two emission peaks were observed at 415 and 450 nm. The emission peaks at 415 and 450 nm could be ascribed to the spin-allowed and spin-forbidden 5d–4f transitions of Yb^{2+} because the

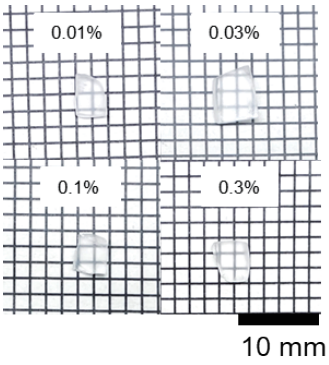

Fig. 1. (Color online) Appearance of LiBr:Yb.

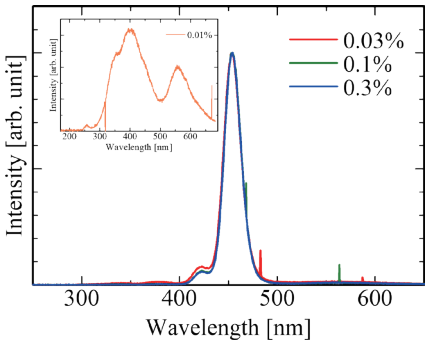

Fig. 2. (Color online) Scintillation spectra under X-ray irradiation.

wavelengths were almost the same as those of NaCl:Yb,[37,38] CsI:Yb,[36] and KBr:Yb.[39] The emission intensity ascribed to spin-allowed transitions was considerably lower than that due to spin-forbidden transitions, and the relative intensity due to spin-allowed transitions decreased as the Yb concentration increased. The emission due to spin-allowed transitions was often observed in high local site symmetries in previous studies.[33,43] Owing to the distortion of the symmetries caused by Yb doping, the relative intensity of spin-allowed transitions possibly decreased. Scintillation decay profiles with different time ranges under pulse X-ray irradiation are illustrated in Fig. 3. Since the 0.01% Yb-doped sample did not show the luminescence due to Yb^{2+}, scintillation decay curves were measured only for the other samples. From the results, the obtained decay time constants were 27–53 ns and 306–310 μs. The fast and slow components were typical values due to spin-allowed and spin-forbidden 5d–4f transitions, respectively, of Yb^{2+} in Yb-doped alkali halides.[36–39]

Pulse height spectra under neutron irradiation from a ^{252}Cf source are presented in Fig. 4. GS20 was used as a reference sample; the *LY* of GS20 was reported to be 6000 ph/n.[25] The shaping times were 10 μs for LiBr:Yb and 2 μs for GS20. All the samples showed a clear neutron peak, and the *LY* was calculated by comparing the peak channel of the neutron peak and the quantum efficiency (*QE*) of PMT at emission wavelength with those of GS20. The *QE*, peak channel (^{252}Cf-P), and *LY* are summarized in Table 1. The 0.03% Yb-doped sample showed the highest *LY* of 3500 ph/n among all the LiBr:Yb. The *LY* was lower than those of not only GS20 but also all commercial scintillators for neutron detection. However, the *LY* might be underestimated because the decay time due to spin-forbidden transitions of Yb^{2+} was too long to completely shape all scintillation signals with the shaping time of 10 μs. Consequently, the *LY* would increase when measured with a longer shaping time. Pulse height spectra under ^{252}Cf neutron and ^{137}Cs γ-ray irradiation of the 0.03% Yb-doped sample and GS20 are shown in Fig. 5. A photoabsorption peak was observed in both the 0.03% Yb-doped sample and GS20. Table 1 shows the peak channel of the photoabsorption peak (^{137}Cs-P), *LY* under ^{137}Cs γ-ray irradiation, and α/γ ratio, assuming that an energy of 4.78 MeV in neutron capture was deposited. The *LY* values of the 0.03% Yb-doped LiBr and GS20 were calculated to be 1900 and 3600 ph/MeV, respectively. In addition, the *α*/*γ* ratio of the 0.03% Yb-doped LiBr was 0.38, which was

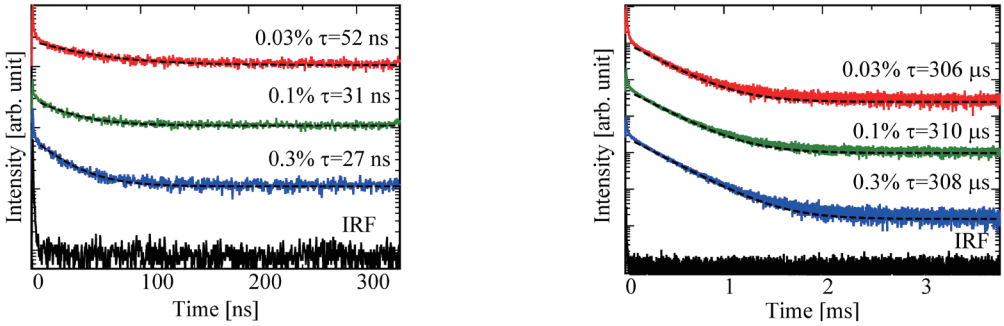

(a) (b)

Fig. 3. (Color online) Scintillation decay profiles under pulse X-ray irradiation in the range of (a) ns and (b) ms.

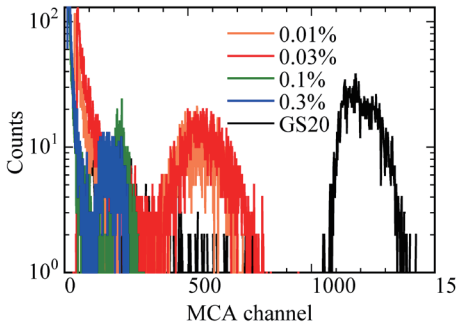

Fig. 4. (Color online) Pulse height spectra of LiBr:Yb and GS20 under neutron irradiation from ^{252}Cf source.

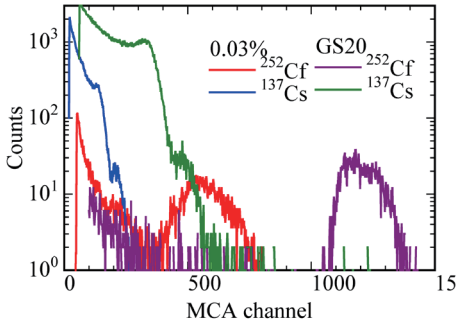

Fig. 5. (Color online) Pulse height spectra of LiBr:0.03%Yb and GS20 under ^{252}Cf neutron and ^{137}Cs γ-ray irradiation.

Table 1
QE, peak channel (P), LY under ^{252}Cf neutron and ^{137}Cs γ-ray irradiation, and α/γ ratio.

Sample	*QE*	^{252}Cf-P (ch)	*LY* (ph/n)	^{137}Cs-P (ch)	*LY* (ph/MeV)	α/γ ratio
0.01%	38.53	538	2700	–	–	–
0.03%	31.02	558	3500	204	1900	0.38
0.1%	31.02	227	1400	–	–	–
0.3%	31.02	180	1100	–	–	–
GS20	38.53	1191	6000	467	3600	0.35

comparable to or higher than that of GS20. According to a previous report on LiBr:Eu,[31] the *LY* and α/γ ratio were 4600 ph/n and 0.37, respectively. Compared with LiBr:Eu, LiBr:Yb showed a lower *LY*, but the α/γ ratio was almost the same.

4. Conclusions

To develop new scintillators for neutron detection, the scintillation properties of LiBr:Yb were evaluated. Two emission peaks were observed at 415 and 450 nm, and decay time constants were 27–52 ns and 306–308 μs. The results indicate the emission origin to be spin-allowed and spin-forbidden 5d–4f transitions of Yb^{2+}. According to the pulse height spectra, the highest *LY*

values were 3500 ph/n and 1900 ph/MeV under ^{252}Cf neutron and ^{137}Cs γ-ray irradiation, respectively, and the α/γ ratio was 0.38. Although the *LY* was lower than that of GS20, the α/γ ratio was comparable to or higher than that of GS20. Since the decay time was too long to completely shape all the scintillation signals, the *LY* might improve when measured with a longer shaping time.

Acknowledgments

This work was supported by JSPS KAKENHI (22H00309, 23K25126, 24K03197, 25K08266, and 25KJ1821), the Cooperative Research Project of the Research Center for Biomedical Engineering, Research Foundation for Electrotechnology of Chubu, and Shimadzu Science Foundation.

References

1 R. T. Kouzes, J. H. Ely, L. E. Erikson, W. J. Kernan, A. T. Lintereur, E. R. Siciliano, D. L. Stephens, D. C. Stromswold, R. M. Van Ginhoven, and M. L. Woodring: Nucl. Instrum. Methods Phys. Res. Sect. A **623** (2010) 1035. https://doi.org/10.1016/j.nima.2010.08.021
2 N. Matsubayashi, H. Tanaka, T. Takata, K. Okazaki, Y. Sakurai, and M. Suzuki: Radiat. Meas. **140** (2021) 106489. https://doi.org/10.1016/j.radmeas.2020.106489
3 A. Nikitin and S. Bliven: IEEE Nucl. Sci. Symp. Med. Imaging Conf. (IEEE, 2010) 1214–1219. https://doi.org/10.1109/NSSMIC.2010.5873961
4 M. Uesaka and H. Kobayashi: Rev. Accel. Sci. Technol. **08** (2015) 181. https://doi.org/10.1142/S1793626815300108
5 J. Als-Nielsen, A. Bahnsen, and W. K. Brown: Nucl. Instrum. Methods **50** (1967) 181. https://doi.org/10.1016/0029-554X(67)90039-0
6 R. T. Kouzes: https://doi.org/10.2172/956899 (May 2009).
7 K. Miyazaki, D. Nakauchi, T. Kato, N. Kawaguchi, and T. Yanagida: Radiat. Phys. Chem. **207** (2023) 110820. https://doi.org/10.1016/j.radphyschem.2023.110820
8 K. Miyazaki, D. Nakauchi, T. Kato, N. Kawaguchi, and T. Yanagida: J. Mater. Sci. Mater. Electron. **33** (2022) 22162. https://doi.org/10.1007/s10854-022-08996-y
9 K. Yamabayashi, K. Okazaki, D. Nakauchi, T. Kato, N. Kawaguchi, and T. Yanagida: Sens. Mater. **36** (2024) 523. https://doi.org/10.18494/SAM4760
10 H. Kimura, H. Fukushima, K. Watanabe, T. Fujiwara, H. Kato, M. Tanaka, T. Kato, D. Nakauchi, N. Kawaguchi, and T. Yanagida: Sens. Mater. **36** (2024) 507. https://doi.org/10.18494/SAM4767
11 M. Ishida, A. Watanabe, H. Kawamoto, Y. Fujimoto, and K. Asai: Sens. Mater. **37** (2025) 607. https://doi.org/10.18494/SAM5482
12 K. Miyazaki, D. Nakauchi, T. Kato, N. Kawaguchi, and T. Yanagida: J. Mater. Sci. Mater. Electron. **34** (2023) 4. https://doi.org/10.1007/s10854-023-10517-4
13 K. Shunkeyev, A. Kenzhebayeva, S. Sagimbayeva, Y. Syrotych, and Y. Zorenko: J. Lumin. **284** (2025) 121308. https://doi.org/10.1016/j.jlumin.2025.121308
14 Y. Endo, K. Ichiba, D. Nakauchi, T. Kato, N. Kawaguchi, and T. Yanagida: Sens. Mater. **36** (2024) 473. https://doi.org/10.18494/SAM4758
15 T. Kato, D. Nakauchi, N. Kawaguchi, and T. Yanagida: Sens. Mater. **36** (2024) 531. https://doi.org/10.18494/SAM4749
16 S. Otake, S. Takase, T. Kato, D. Nakauchi, N. Kawaguchi, and T. Yanagida: Sens. Mater. **37** (2025) 519. https://doi.org/10.18494/SAM5433
17 K. Okazaki, D. Nakauchi, A. Nishikawa, T. Kato, N. Kawaguchi, and T. Yanagida: Sens. Mater. **36** (2024) 587. https://doi.org/10.18494/SAM4753
18 S. Muneta, N. Kawano, D. Nakauchi, T. Kato, K. Okazaki, K. Ichiba, T. Kunikata, A. Nishikawa, K. Miyazaki, F. Kagaya, K. Shinozaki, and T. Yanagida: Sens. Mater. **37** (2025) 509. https://doi.org/10.18494/SAM5441

19 Y. Takebuchi, A. Masuno, D. Shiratori, K. Ichiba, A. Nishikawa, T. Kato, D. Nakauchi, N. Kawaguchi, and T. Yanagida: Sens. Mater. **36** (2024) 579. https://doi.org/10.18494/SAM4751
20 K. Miyajima, A. Nishikawa, T. Kato, D. Nakauchi, N. Kawaguchi, and T. Yanagida: Sens. Mater. **37** (2025) 481. https://doi.org/10.18494/SAM5436
21 D. Nakauchi, H. Kimura, D. Shiratori, T. Kato, N. Kawaguchi, and T. Yanagida: Sens. Mater. **36** (2024) 573. https://doi.org/10.18494/SAM4750
22 C. D. Bass, E. J. Beise, H. Breuer, C. R. Heimbach, T. J. Langford, and J. S. Nico: Appl. Radiat. Isot. **77** (2013) 130. https://doi.org/10.1016/j.apradiso.2013.03.053
23 K. Miyazaki, D. Nakauchi, T. Kato, N. Kawaguchi, and T. Yanagida: Opt. Mater. **146** (2023) 114557. https://doi.org/10.1016/j.optmat.2023.114557
24 K. Hasegawa, Y. Nakabayashi, A. Watanabe, H. Kawamoto, Y. Fujimoto, and K. Asai: J. Mater. Sci. Mater. Electron. **36** (2025) 636. https://doi.org/10.1007/s10854-025-14718-x
25 C. W. E. Van Eijk: Radiat. Meas. **38** (2004) 337. https://doi.org/10.1016/j.radmeas.2004.02.004
26 Y. Yehuda-Zada, K. Pritchard, J. B. Ziegler, C. Cooksey, K. Siebein, M. Jackson, C. Hurlbut, Y. Kadmon, Y. Cohen, R. M. Ibberson, C. F. Majkrzak, N. C. Maliszewskyj, I. Orion, and A. Osovizky: Nucl. Instrum. Methods Phys. Res. Sect. A **892** (2018) 59. https://doi.org/10.1016/j.nima.2018.02.099
27 V. Popov and P. Degtiarenko: IEEE Nucl. Sci. Symp. Conf. (IEEE, 2010) 1819–1822. https://doi.org/10.1109/NSSMIC.2010.5874089
28 J. Glodo, R. Hawrami, and K. S. Shah: J. Cryst. Growth **379** (2013) 73. https://doi.org/10.1016/j.jcrysgro.2013.03.023
29 R. B. Murray: Nucl. Instrum. **2** (1958) 237. https://doi.org/10.1016/0369-643X(58)90035-5
30 T. Yanagida, N. Kawaguchi, Y. Fujimoto, K. Fukuda, Y. Yokota, A. Yamazaki, K. Watanabe, J. Pejchal, A. Uritani, T. Iguchi, and A. Yoshikawa: Opt. Mater. **33** (2011) 1243. https://doi.org/10.1016/j.optmat.2011.02.016
31 K. Miyazaki, D. Nakauchi, T. Kato, N. Kawaguchi, and T. Yanagida: J. Lumin. **274** (2024) 120712. https://doi.org/10.1016/j.jlumin.2024.120712
32 M. Suta and C. Wickleder: Adv. Funct. Mater. **27** (2017). https://doi.org/10.1002/adfm.201602783
33 K. Mizoi, M. Arai, Y. Fujimoto, D. Nakauchi, M. Koshimizu, T. Yanagida, and K. Asai: J. Ceram. Soc. Jpn. **129** (2021) 20225. https://doi.org/10.2109/jcersj2.20225
34 N. Wantana, P. Q. Vuong, N. T. Luan, H. J. Kim, N. D. Quang, C. Mutuwong, Y. Tariwong, P. Pakawanit, S. Kothan, and J. Kaewkhao: Radiat. Phys. Chem. **224** (2024) 112022. https://doi.org/10.1016/j.radphyschem.2024.112022
35 C. van Aarle, K. W. Krämer, and P. Dorenbos: J. Lumin. **238** (2021) 118257. https://doi.org/10.1016/j.jlumin.2021.118257
36 D. Sofich, A. Myasnikova, A. Bogdanov, V. Pankratova, V. Pankratov, E. Kaneva, and R. Shendrik: Crystals **14** (2024) 500. https://doi.org/10.3390/cryst14060500
37 T. Tsuboi, H. Witzke, and D. S. McClure: J. Lumin. **24** (1981) 305. https://doi.org/10.1016/0022-2313(81)90278-7
38 T. Tsuboi, D. S. McClure, and W. C. Wong: Phys. Rev. B **48** (1993) 62. https://doi.org/10.1103/PhysRevB.48.62
39 A. Seguchi, K. Miyazaki, D. Nakauchi, T. Kato, N. Kawaguchi, and T. Yanagida: Opt. Mater. **168** (2025) 117406. https://doi.org/10.1016/j.optmat.2025.117406
40 D. Nakauchi, Y. Fujimoto, T. Kato, N. Kawaguchi, and T. Yanagida: Jpn. J. Appl. Phys. **60** (2021) 2. https://doi.org/10.35848/1347-4065/ac15af
41 T. Yanagida, K. Kamada, Y. Fujimoto, H. Yagi, and T. Yanagitani: Opt. Mater. **35** (2013) 2480. https://doi.org/10.1016/j.optmat.2013.07.002
42 T. Yanagida, Y. Fujimoto, T. Ito, K. Uchiyama, and K. Mori: Appl. Phys. Express **7** (2014) 4. https://doi.org/10.7567/APEX.7.062401
43 M. Suta, T. Senden, J. Olchowka, M. Adlung, A. Meijerink, and C. Wickleader: Phys. Chem. Chem. Phys. **19** (2017) 7188. https://doi.org/10.1039/C7CP00581D